J Electron Test (2010) 26:499–511
DOI 10.1007/s10836-010-5171-x

Fault Models for Quantum Mechanical Switching Networks

Jacob D. Biamonte · Jeff S. Allen · Marek A. Perkowski

Received: 22 August 2005 / Accepted: 3 September 2010 / Published online: 16 November 2010

Abstract In classical test and verification one develops a test set separating a correct circuit from a circuit containing any considered fault. Classical faults are modelled at the logical level by fault models that act on classical states. The stuck fault model, thought of as a lead connected to a power rail or to a ground, is most typically considered. A classical test set complete for the stuck fault model propagates both binary basis states, 0 and 1, through all nodes in a network and is known to detect many physical faults. A classical test set complete for the stuck fault model allows all circuit nodes to be completely tested and verifies the function of many gates. It is natural to ask if one may adapt any of the known classical methods to test quantum circuits. Of course, classical fault models do not capture all the logical failures found in quantum circuits. The first obstacle faced when using methods from classical test is developing a set of realistic quantum-logical fault models (a question which we address, but will likely remain largely open until the advent of the first quantum computer). Developing fault models to abstract the test problem away from the device level motivated our study. Several results are established. First, we describe typical modes of failure present in the physical design of quantum circuits. From this we develop fault models for quantum binary quantum circuits that enable testing at the logical level. The application of these fault models is shown by adapting the classical test set generation technique known as constructing a fault table to generate quantum test sets. A test set developed using this method will detect each of the considered faults.

Keywords Testing · Fault modeling · Diagnostics · Error-checking · Reversible computers · Quantum computers · Formal test and verification

Responsible Editor: V. D. Agrawal

J. D. Biamonte · J. S. Allen · M. A. Perkowski
Portland State University, 1900 SW Fourth Avenue,
P.O. Box 751, Portland, OR 97201, USA

Present Address:
J. D. Biamonte (✉)
Oxford University Computing Laboratory, Wolfson
Building, Parks Road, Oxford, OX1 3QD, UK
e-mail: jacob.biamonte@gmail.com

1 Introduction

Test methods in use today began to be developed in the 1960's anticipating circuit sizes that would make exhaustive test methods intractable. Classical test theory attempts to determine if a given circuit is or is not functional [30, 31]. This is accomplished by testing a circuit in order to determine if any of the logical failures modelled by the set of considered fault models are present. Fault models are typically inspired by physical failures but may also represent abstractions that enable the creation of test sets detecting an abundance of actual physical faults.

Applying established methods of classical circuit test [29, 37] theory to test quantum circuits has attracted interest in recent times [51], with results reported in [8, 19, 46, 47]. The present work attempts to present adequate justification for some of the fault models already considered, and also defines several new fault models for future test pattern generation studies.

Experimental physicists who build quantum circuits have not experienced much need to research optimized

testing methods due to the size of the currently attainable qubit count so the quantum test problem remains of theoretical interest today [3, 20, 24, 25, 27, 32, 35, 52]. In Appendix B we review both this currently practiced (exhaustive) approach to the quantum circuit test problem as well as distance measures to compare quantum states.

A quantum circuit is built out of gates and these are connected using nodes and wires (we can think of this as a logical network, or physically as say an optical quantum circuit). If so many as a single gate, single node or a wire is broken, the quantum circuit is unusable. This is in contrast to quantum errors corrected by control codes [33]. The possibility to construct quantum networks completely free of faults is generally assumed since error correction relies on fault free networks. It is therefore important to test the inter-connectivity of the network nodes, wires and gates in an attempt to locate faults. This work addresses this problem by justifying several logical fault models dependent on the structure of quantum switching networks. Test sets complete for logical fault models determine if any considered fault is present in the interconnections or the gates of a quantum network. In practice, test sets are developed to detect all of the most common faults.

Classically, one defines a testability measure as a product of observability and controllability. The controllability of testing a circuit corresponds to propagating a specific input test vector through a network, such that it will map a test vector to a place of fault. This represents an added challenge in the case of testing quantum circuits, since inputs may become entangled and faults may occur non-deterministically. Furthermore, depending on the measurement basis chosen, certain faults may not be detectable. With these limitations in mind and after defining our notation next, in Section 2, we present a set of quantum fault models (Sections 3–8). The presence of even one of these faults will make a quantum circuit unusable so we show how to develop test sets in Appendix C under the assumption that the fault-tolerant quantum circuit [33] under test contains at most one of the considered faults. We further assume that each quantum circuit is executed multiple times and that the output is averaged over, using a majority voting procedure.[1]

[1]The Chernoff Bound asserts that polynomial many repetitions of independent samples will converge exponentially fast to the true mean. See for instance Chapter 4 of the text book by R. Motwani and P. Raghavan: *Randomized Algorithms*, Cambridge University Press (1995).

2 Background and Notation

Let us define the state $\sqrt{2} \cdot |\pm\rangle = |0\rangle \pm |1\rangle$ and mention that the notational conventions from the textbook by Nielsen and Chuang [41] are used.[2] We let $\hat{Z}$ be the standard observable in the computational basis and $\hat{X}$ be an observable in the conjugate basis [36].[3]

2.1 The Types of Quantum Circuits Considered

The goal of test is to develop logical fault models, which capture functional aspects of circuits. We will present a set of physically motivated quantum fault models for quantum circuits built from $k-$CN gates [41]. At this early stage, to separate the general from the particular, a focus is made on error and fault models that are independent of implementation.

We have developed the fault models used in this work by considering examples from several current technologies such as liquid state nuclear magnetic resonance spectroscopy (NMR)[4] and optical quantum computation are used. Although the NMR implementation is not scalable, it is currently the most successful [53]. Optical quantum computation has the potential of scalability and has recently made progress. For instance, in 2003 O'Brien et al. [43] successfully demonstrated an optical quantum CN gate. This gate was improved and further characterized in 2004 by both O'Brien et al. [44] and White et al. [56].

Remark 2.1 (*Considered Quantum Circuits*) At this early stage, the logical fault models we consider should be closest to a quantum computer implementation in which there is an actual physical circuit with components). This is true for some quantum technologies (e.g. such as optical), this is however not true for several other important technologies including trapped-ion and NMR.

[2]Note to readers new to quantum circuits: The background to read this paper appears in Chapters 1, 3 and 8 of the text book [41]. Course lecture notes accompanying [41] can be found online [45].

[3]The conjugate basis is formed by measuring $\hat{Z}$ after rotating all qubits with a Hardamard transform [41].

[4]See Jones [22] for an introduction geared towards those new to NMR Quantum Computing.

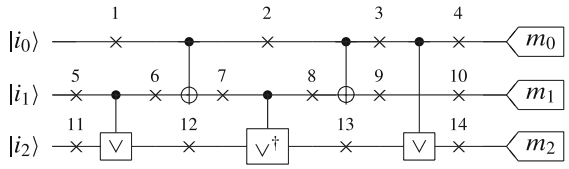

Fig. 1 2−CN gate with 14 gate external error locations numbered above an "×" and five possibly erroneous gates. The construction of the gates used in this circuit are outlined in Section 6

2.2 Testing Definitions

In quantum error correcting codes, fault locations are between circuit stages,[5] and have quantifiable error probabilities [33]. For example, consider the five stage circuit shown in Fig. 1. The numbered locations of possible gate external faults are illustrated by placing an "×" on the lines representing qubits. The five gates, initial states ($|\psi_0\rangle$, $|\psi_1\rangle$, $|\psi_2\rangle$) and measurements (M_0, M_1, M_2) may also contain errors.

Definition 2.2 Error location: the wire locations between stages as well as any node or gate in a given network represent error locations.

Definition 2.3 Gold circuit: an ideal quantum circuit denoted GC. Typically a non-ideal quantum circuit is denoted QC.

Definition 2.4 Fault set: denote by F_q a set containing all considered faults assumed to impact QC.

Definition 2.5 Quantum test set: a sequence of initial states $|\psi_i\rangle$ and corresponding measurements M_i used to distinguish QC possibly perturbed by any $f \in F_q$ from a gold circuit GC.

Complete fault coverage occurs if executing a test set can determine that all of the considered faults are not present in a given circuit.

Definition 2.6 Fault coverage: denote by QC a quantum circuit possibly perturbed by any element of a set of faults $f \in F_q$ and a test set T complete for all $f \in F_q$. Fault Coverage occurs for fault f by experimentally running $t \subseteq T$ that detects f. A quantum test set that detects all considered faults is a complete test set.

Since even the presence of one of the faults considered in this work would make a quantum circuit unusable, when developing quantum test sets in Section 9, we assume that the fault-tolerant quantum circuit [33] under test contains at most one of the considered faults. This assumption is called the *quantum single fault model*. Classically, test sets complete for single faults are known to detect the presence of multiple faults [38]. Whether or not the quantum single fault model dominates multiple quantum faults is left as an open problem.

Definition 2.7 Quantum single fault model: consider the quantum fault set F_q. In the quantum single fault model, test plans are developed to detect all $f \in F_q$ assuming that at most one fault, f, is present in QC.

Remark 2.8 (*Validity of the Single Fault Assumption*) The single-fault assumption, or Single Fault Model is considered in this work. This means that test patterns are developed to detect only single faults occurring at one time. This assumption is known to work well for conventional circuits (e.g. the test sets complete for the single fault model detect multiple faults) [38]. This assumption is currently unverified for quantum circuits.

Definition 2.9 Pauli matrices:

$$\sigma_x = |1\rangle\langle 0| + |0\rangle\langle 1|, \qquad \sigma_y = i|0\rangle\langle 1| - i|1\rangle\langle 0|,$$
$$\sigma_z = |0\rangle\langle 0| - |1\rangle\langle 1| \qquad \text{and} \qquad \sigma_i = |0\rangle\langle 0| + |1\rangle\langle 1|. \tag{1}$$

Definition 2.10 Rotation matrices:

$$R_x(\theta) = \begin{pmatrix} \cos(\theta/2) & -i\cdot\sin(\theta/2) \\ -i\cdot\sin(\theta/2) & \cos(\theta/2) \end{pmatrix},$$
$$R_y(\theta) = \begin{pmatrix} \cos(\theta/2) & -\sin(\theta/2) \\ \sin(\theta/2) & \cos(\theta/2) \end{pmatrix} \qquad \text{and}$$
$$R_z(\phi) = e^{-i\phi/2}|0\rangle\langle 0| + e^{i\phi/2}|1\rangle\langle 1|. \tag{2}$$

With the basic definitions behind us, the coming sections discuss gate level failures and introduce several requirements that a quantum test set must satisfy. Each requirement must be satisfied for a test set to be complete and cover all considered faults.

[5] In particular see [33] where Knill, Laflamme, and Zurek justified the idea of an error location for the purpose of quantum error correction.

3 Faults (Errors) Modeled with Pauli Matrices

The Pauli-matrices give rise to errors or faults that are correctable using quantum error correction. This is in contrast to several of the non-reversible (non-unitary) faults we consider at later stages in this work.

Definition 3.1 Pauli fault model: The addition of an unwanted Pauli matrix f in quantum network QC, at error location l and with placement probability p.

The unavoidable entanglement between a quantum processor and the outside world is described by many authors as, "*coupling to an initially independent environment* [34]." This is a primary source of decoherence. A large amount of research has been devoted to removing the local effects of decoherence by quantum error correcting codes. Consequently, what are known as error models are found in the quantum error correcting code literature [1, 6, 7, 49, 50]. The most investigated error model is the "*independent depolarizing error* [33]." This model has the effect of completely randomizing a given qubit with some probability [41] and "*...error models designed to control depolarizing errors apply to all independent error models* [34]." These codes are designed to correct unwanted single qubit σ_x, σ_y and σ_z rotations. The following is a list of the range of errors modeled assuming Pauli Faults, with some supporting references:

- Depolarizing channels [34, 41]
- Amplitude dampening [33, 41]
- Phase damping [28, 41]
- Phase-flips [28, 33, 41]
- Bit-flips [33, 41]
- Initialization inaccuracies [4, 28]
- Measurement inaccuracies [10, 21, 57]

In addition to noise, repeatable errors in a physical construction lead to another class of faults addressed in the literature. These are known as *systematic errors* and are again modeled by Pauli Faults. Systematic errors are closer to the types of errors that classical test engineers refer to as faults. These errors are described by Cummins and Jones as, "*arising from the reproducible imperfections in the apparatus used to implement quantum computations* [13]." The most common systematic errors are given in the following list, again with supporting references:

- Pulse length errors [9, 13, 14, 42]
- Off-resonance effects [9, 13, 54]
- Refocusing errors [23, 54]

Quantum Fault Model 1 (Pauli Fault Model 1) *A bit flip (σ_x or σ_y) at any error location must be detectable.*

It turns out that these faults are very easy to detect in quantum switching circuits. The following Theorem 3.2 states that any σ_x or σ_y fault occurring in a network built from $k-$CN gates is detectable with any computational basis input state. In addition, a reversible system preserves information and one can show that the probability of detection for fault f observable with $\hat{A}$, is directly related to the probability of f's presence.

Theorem 3.2 *Pauli Faults σ_x and σ_y impacting an n qubit network QC comprised of $k-CN$ gates at any gate external error location are detected with any basis input state $|s\rangle$ given an observable in the computational basis.*

Proof Any reversible binary quantum network QC of l qubits and n stages bijectively maps each input $|s\rangle$ to a unique output $|s'\rangle$. Each gate $g \in QC$ is reversible, thus any stage n acting on input vector $|s\rangle$ corresponds to exactly one output vector at the $(n+1)^{\text{th}}$ stage. A qubit flip (f_p) occurs before or after any stage n on any wire l, changing the output from the previous stage (and input to the next). Any σ_x or σ_y fault is therefore detectable based on the properties of reversibility [59] with any basis state input $|k\rangle$ given an observable in the computational basis. □

From Theorem 3.2 it follows that any test set that contains a basis state input and corresponding measurement in the computational basis dominates a test set complete for Pauli Fault Model 1. This desirable property does not hold for σ_z phase faults.

Quantum Fault Model 2 (Pauli Fault Model 2) *A phase flip (σ_z) at any error location must be detectable.*

4 Initialization Faults

Initialization faults were discussed in detail by Kak [28], and addressed experimentally in [4, 54]. Because initialization accuracies relate to a machine's ability to perform a task (such as not altering the initial state population in NMR [54]), one can develop a test set to determine if the machine is impacted by any of the considered initialization faults. We model these faults using Definition 4.1.

Definition 4.1 Initialization error: A qubit with an initial state impacted by an unwanted rotation $R_n(\theta)$

where $n \in \{x, y, z\}$, *or* a qubit that is only correctly prepared in one basis state and not the other.

From Definition 4.1, examples of how initialization faults spread are shown in Fig. 2. The fault in Fig. 2b could occur when the desired initial state is $|01c\rangle$ and the top qubit is inverted ($|c\rangle \rightarrow |\bar{c}\rangle$) resulting in the state: $\cos\theta\,|01c\rangle - i\sin\theta\,|11\bar{c}\rangle$. After being acted on by the 2−CN gate, the state of the system becomes $\cos\theta\,|01c\rangle - i\sin\theta\,|11c\rangle$. There is now a probability of $(\sin\theta)^2$ that an incorrect value will be measured.

A similar scenario holds for Fig. 2c—in this case the center qubit is impacted by an initialization fault as opposed to the top qubit in Fig. 2b. In Fig. 2d the desired initial state is $|-\,-\,+\rangle$, however a fault impacts the bottom qubit flipping its phase—changing the initial state to $|-\,-\,-\rangle$. Now the 2−CN gate will entangle the state of the system incorrectly, resulting in state $(|00\rangle - |01\rangle - |10\rangle - |11\rangle)\,|-\rangle$. This fault can be detected with a test set detecting unwanted instances of the Pauli Faults. A second type of initialization error will now be discussed.

Generally, there exists a certain set of states left invariant under a quantum operation [41]. For example, qubit preparation may be altered with a form of amplitude dampening. Thus, a faulty qubit might only allow preparation into one state. A qubit that can only be prepared in density state $|0\rangle\langle 0|$ is modeled with the following operation elements:

$$E_0 = |0\rangle\langle 0| + \left(\sqrt{1-\gamma}\right)|1\rangle\langle 1|$$

$$E_1 = |0\rangle\langle 0| + \left(\sqrt{\gamma}\right)|1\rangle\langle 1|$$

Consider a register prepared in density state $\rho = \rho_0 \otimes \ldots \otimes \rho_k \otimes \ldots \otimes \rho_n$. The kth qubit is desired to start the computation in an arbitrary state, expressed as:

$$\rho = \rho_0 \otimes \ldots \otimes \begin{pmatrix} \alpha^2 & \alpha\beta^* \\ \beta\alpha^* & \beta^2 \end{pmatrix} \otimes \ldots \otimes \rho_n$$

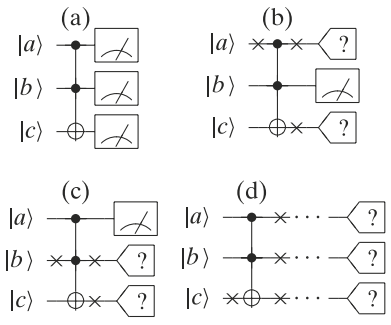

Fig. 2 Initialization errors impacting a 2−CN gate: **a** correct circuit, **b–d** various initialization errors

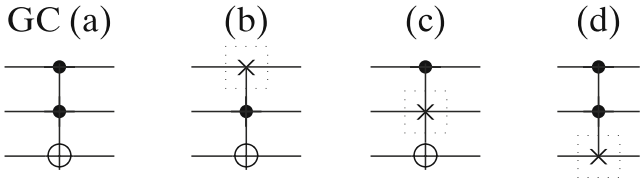

Fig. 3 2−CN gate and phase faults: **a** gold circuit, **b** weak top control, **c** weak second control, **d** weak gate

The unwanted impact of initial state dampening is expressed as: $\mathcal{E}(\rho) = \sum_k \sigma_i \otimes \ldots \otimes E_k \otimes \ldots \otimes \sigma_i \cdot \rho \cdot \sigma_i \otimes \ldots \otimes E_k^\dagger \otimes \ldots \otimes \sigma_i$. This results in the state:

$$\rho' = \rho_0 \otimes \ldots \otimes \begin{pmatrix} \alpha^2 + \gamma\beta^2 & \alpha\beta^*\sqrt{1-\gamma} \\ \beta\alpha^2\sqrt{1-\gamma} & \beta^2(1-\gamma) \end{pmatrix} \otimes \ldots \otimes \rho_n.$$

The projection of the kth qubit's state onto the basis $|1\rangle\langle 1|$ is forced into basis state $|0\rangle\langle 0|$ and the off diagonal terms are suppressed (both based on some parameter γ). Similarly, a faulty qubit might only allow preparation into density state $|1\rangle\langle 1|$. A test set complete for Quantum Fault Model 3 determines if any qubit can only be correctly prepared in one basis state and not the other.

Quantum Fault Model 3 (Initialization Fault Model) *Each qubit must be initialized in both basis states* $|0\rangle$ *and* $|1\rangle$.

5 Lost Phase Faults

Remark 5.1 (*Background on Quantum Search and on Oracles*) Several outstanding introductions to quantum search and oracles can be found in the literature. An excellent starting place for background reading is be the book [41] (and the citations therein).

Shenvi, Brown and Whaley [49] studied Grover's search algorithm [41] impacted by random phase errors in the oracle.[6] They model errors by applying unwanted phase shifts $\pm\epsilon$ to the state of a quantum register marked by an oracle: $\mathcal{O} : |k\rangle \longrightarrow e^{i\pi\cdot(f(k)\pm\epsilon)}\,|k\rangle$. Several references including [49] call this a "*phase-kick-error*." Figure 3b–d illustrate faulty

[6] Grover's original algorithm has recently been updated by Grover [18]. Although this new "*Fixed Point Algorithm*" is more robust, it is still subject to phase errors. The algorithm has been experimentally verified by Xiao and Jones [58], systematic errors in the physical implementation were briefly explored. B. Reichardt and L. Grover have also recently developed methods of systematic error correction for this new algorithm [48].

Table 1 The impact phase faults from Fig. 3 have on input state $|++-\rangle$

Term	Initial	GC (a)	(b)	(c)	(d)
$\|000\rangle$	+1	+1	+1	+1	+1
$\|001\rangle$	−1	−1	−1	−1	−1
$\|010\rangle$	+1	+1	−1	+1	+1
$\|011\rangle$	−1	−1	+1	−1	−1
$\|100\rangle$	+1	+1	+1	−1	+1
$\|101\rangle$	−1	−1	−1	+1	−1
$\|110\rangle$	+1	−1	−1	−1	+1
$\|111\rangle$	−1	+1	+1	+1	−1

The *first column* shows the phase of each term before being acted on by the circuit. The column *GC (a)* shows the correct phase relative phase of each term in the superposition. The remaining columns (*b–d*) show how the phase changes depending on the fault present

controls that have phase kick-back faults. A correct 3−CN gate will map an input state $|++\rangle|-\rangle$ to output state $(|000\rangle + |001\rangle + |010\rangle + |011\rangle + |100\rangle + |101\rangle + |110\rangle - |111\rangle)|-\rangle$. Each term in the superposition that activates the gate will undergo a phase shift of $|n\rangle \longrightarrow e^{i\pi}|n\rangle$. If the fault in Fig. 3b is present, the circuit's output is $(|000\rangle + |001\rangle + |010\rangle - |011\rangle + |100\rangle + |101\rangle + |110\rangle - |111\rangle)|-\rangle$. In this case, relative phase shifts occur on both states $|011\rangle$ and $|111\rangle$ since those activate the gate when the top control is broken. Another type of fault is phase damping. This is a noise process altering relative phases between quantum states [41]. A test set complete for the Lost Phase Fault Model determines if the faults described above are present in a given quantum circuit (Table 1).

Quantum Fault Model 4 (Lost Phase Fault Model[7]) *Consider the circuit input as* $H^{\otimes n} \cdot |x_1, x_2, ..., x_n\rangle$ *with* $x_i \in \{0, 1\}$ *and measurement of* $\hat{X}$. *Given freedom in the choice of input vector* $x_1, x_2, ..., x_n$ *a circuit must be shown to have no missing single control or single gate.*

To show that the considered phase faults are not present in the network we place Hardamard gates at the start and at the end of the circuit under test and measure $\hat{Z}$. Let us denote the circuit under test as C_i where subscript i signifies that impact of the ith considered fault. We will define the input as $\rho = |x_1x_2x_3\rangle\langle x_1x_2x_3|$ with x_1, x_2 and x_3 in $\{0, 1\}$. The goal is to show separation of GC from each of the considered faults where $\rho' = H^{\otimes 3} \cdot C_i \cdot H^{\otimes 3} \cdot \rho \cdot H^{\otimes 3} \cdot C_i^{\dagger} \cdot H^{\otimes 3}$ allows freedom in the choice of the input ρ. Here we choose $\rho = |001\rangle\langle 001|$ and note that for fault (b): $\mathrm{tr}(|100\rangle\langle 100| \cdot \rho') = 1$, for fault (c): $\mathrm{tr}(|101\rangle\langle 101| \cdot \rho') = 1$ and for fault (d): $\mathrm{tr}(|001\rangle\langle 001| \cdot \rho') = 1$. For GC $\mathrm{tr}(|001\rangle\langle 001| \cdot \rho') = \mathrm{tr}(|100\rangle\langle 100| \cdot \rho') = \mathrm{tr}(|101\rangle\langle 101| \cdot \rho') = \mathrm{tr}(|111\rangle\langle 111| \cdot \rho') = 1/4$.

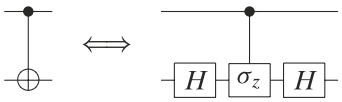

Fig. 4 CN gate constructed with elementary building blocks [26]. The H gate $(H = iR_y(\pi/2)R_z(\pi))$ is given as $H = \frac{1}{\sqrt{2}}(|0\rangle + |1\rangle)\langle 0| + \frac{1}{\sqrt{2}}(|0\rangle - |1\rangle)\langle 1|$ and the center controlled phase shift gate (CZ_i) is given in Eq. 3

6 Faded Control Faults

The building blocks needed to implement any quantum algorithm with NMR can be based on single spin rotations and CN gates [54]. CN gates are realized using a scheme illustrated in Fig. 4. To test the considered 2−CN gate for the considered phase faults one must show separation in the above quantities (Table 2). The

Table 2 Fault table for 2−CN gate with (b) missing top control and (c) missing bottom control

Input	GC (a)	(b)	(c)
$\|000\rangle$	$\|000\rangle$	$\|000\rangle$	$\|000\rangle$
$\|001\rangle$	$\|001\rangle$	$\|001\rangle$	$\|001\rangle$
$\|010\rangle$	$\|010\rangle$	$\|011\rangle$	$\|011\rangle$
$\|011\rangle$	$\|011\rangle$	$\|010\rangle$	$\|010\rangle$
$\|100\rangle$	$\|100\rangle$	$\|100\rangle$	$\|101\rangle$
$\|101\rangle$	$\|101\rangle$	$\|101\rangle$	$\|100\rangle$
$\|110\rangle$	$\|111\rangle$	$\|111\rangle$	$\|111\rangle$
$\|111\rangle$	$\|110\rangle$	$\|110\rangle$	$\|110\rangle$

A test set complete for this fault table is as follows: to separate GC from (b) and (c) measure $\hat{Z}$ for the following inputs $|01\star\rangle$ and $|10\star\rangle$, with $\star\{0, 1\}$

[7]This fault model was first presented at SPIE 2004. It was published in J.D. Biamonte, M. Jeong , J-S. Lee and M.A. Perkowski *Extending classical test to quantum,* Proc. of SPIE Fluctuations and Noise in Photonics and Quantum Optics III, Vol. 5842, p. 194 (2005). Shortly thereafter (independently) a similar version appeared in [19].

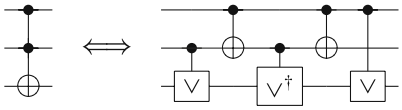

Fig. 5 2−CN gate constructed with elementary building blocks

center gate is a CZ gate and is built using a ϕ gate with angle π (see [26], Section 3.1 Eqn. 34):

$$CZ_i = |00\rangle\langle 00| + |01\rangle\langle 01| + |10\rangle\langle 10| + e^{i\pi}|11\rangle\langle 11|. \tag{3}$$

In any physical implementation, the CZ_i gate might deviate according to our ability to apply phase $e^{i\phi}$ correctly to term $|11\rangle\langle 11|$. This can be represented as:

$$CZ_r = |00\rangle\langle 00| + |01\rangle\langle 01| + |10\rangle\langle 10| + e^{i\phi}|11\rangle\langle 11|. \tag{4}$$

An ideal CN gate creates the following mapping: $CN_i : |10\rangle \longrightarrow |11\rangle$. If the CZ gate applies a phase at the wrong angle ϕ, the mapping becomes: $CN_r : |10\rangle \longrightarrow (1+e^{i\phi})|10\rangle + (1-e^{i\phi})|11\rangle$. The fidelity[8] between the real and ideal CN gate with input $|10\rangle$ is:

$$F(CN_i|10\rangle\langle 10|CN_i^\dagger, CN_r|10\rangle\langle 10|CN_r^\dagger) = \frac{1}{2}(1-\cos\phi).$$

Another gate constructed using a ϕ gate with angle $\pi/2$ [26] is known as the CV gate. The V gate is given as:

$$\vee = |\vee_0\rangle\langle 0| + |\vee_1\rangle\langle 1|, \tag{5}$$

where $|\vee_0\rangle = (1+i)|0\rangle + (1-i)|1\rangle$ and $|\vee_1\rangle = (1-i)|0\rangle + (1+i)|1\rangle$. The CN and CV gates may be combined to create 2−CN gates as shown in Fig. 5. It turns out that by adjusting ϕ, nth root of NOT gates can be constructed [5]. These can be used to build any k−CN gate (for instance, by setting $\phi = \pm\pi/4$ the 4th root of NOT gates can be created and used to build the 3−CN gates in this paper).

Test sets complete for the faded control fault model introduced below must turn each gate on by concurrently activating all controls [2]. These test sets also determine if each control can be turned off properly.

[8]See Appendix B for an explanation of the fidelity.

Fig. 6 The truth table for 2−CN gate and the impact of forced gate faults: the column denoted *input* shows the respective input combinations possible. Columns denoted *a* and *b* show the circuit's response given the presence of faults from Fig. 8a and b, respectively

input	GC	a	b
$\|000\rangle$	000	000	000
$\|001\rangle$	001	001	001
$\|010\rangle$	010	010	010
$\|011\rangle$	011	011	011
$\|100\rangle$	100	100	100
$\|101\rangle$	101	101	101
$\|110\rangle$	111	110	111
$\|111\rangle$	110	110	111

A test set complete for the Faded Control Fault Model tests a controls' function with the target in a basis state. It also tests the controls' impact on both activating and non-activating states.

Quantum Fault Model 5 (Faded Control Fault Model) *For the target acting on basis state $|0\rangle$ or $|1\rangle$: All controls must be activated concurrently and each control must be addressed with a non-activating state.*

7 Forced Gate Faults

Forced gate faults are non-unitary. An example of a non-unitary operation is a gate that when activated applies an "*amplitude dampening process* [41]" to the target bit (a type of relaxation process [54]). A test set complete for Quantum Fault Model 6 forces the gate to act on both a $|0\rangle$ and a $|1\rangle$ to uniquely show that this considered fault is not present. This can be seen further by examining the Truth Table in Figs. 6 and 7. The Forced Gate Fault model is given in Fig. 8.

input	a	b
$\|000\rangle$	0	0
$\|001\rangle$	0	0
$\|010\rangle$	0	0
$\|011\rangle$	0	0
$\|100\rangle$	0	0
$\|101\rangle$	0	0
$\|110\rangle$	1	0
$\|111\rangle$	0	1

Fig. 7 Fault table for 2−CN Gate perturbed by the forced gate faults given in Fig. 8. Each binary entry in the fault table corresponds to a single test (*row*) and a single fault (*column*). Tests are labeled $|000\rangle$ to $|111\rangle$ and faults are labeled *a* and *b*, as shown in Fig. 8a and b. A *1* in the table corresponds to a given test (*row*) detecting a given fault (*column*)

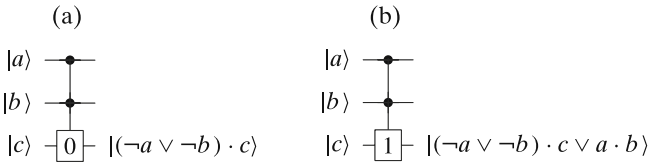

Fig. 8 Forced gate faults: **a** 2−CN gate that correctly acts on a $|1\rangle$ by changing the state to $|0\rangle$, **b** 2−CN gate that correctly acts on a $|0\rangle$ by changing the state to $|1\rangle$ (In both of these cases, we consider binary inputs.)

Quantum Fault Model 6 (Forced Gate Fault Model) *Each target must separately act on basis state inputs* $|0\rangle$ *and* $|1\rangle$.

8 Measurement Faults

Certain types of measurement faults can be caused from a "*limitation in the sensitivity of a measurement apparatus* [10]." Measurement faults are often modelled by the Pauli Fault Model. For example, to project (measure) the state of a photon one places a slit in front of a photo detector. Polarization states inline with the slit will be allowed to reach the photo detector and the angle of the slit is subject to error [21]. Aside from the Pauli Fault Model already considered, a faulty measurement instrument is modelled as a probe that couples to a qubit and consistently returns an a certain value. In Fig. 9 the single measurement fault model is illustrated by placing a faulty measurement gate at the output of the circuit. The truth table derived from Fig. 9 is shown in Fig. 10. The corresponding fault table if given in Fig. 11. Test sets complete for the Measurement Fault Model 7 detect the faults defined below in Definition 8.1.

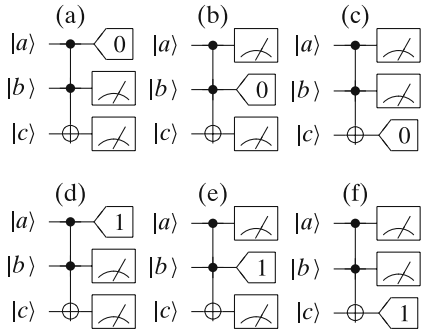

Fig. 9 Measurement errors: **a–c** illustrate measurement faults that statistically favor *logic-zero*; **d–f** contain measurement faults statistically favoring *logic-one*

input	GC	a	b	c	d	e	f
$\|000\rangle$	000	000	000	000	100	010	001
$\|001\rangle$	001	001	001	000	101	011	001
$\|010\rangle$	010	010	000	010	110	010	011
$\|011\rangle$	011	011	001	010	111	011	011
$\|100\rangle$	100	000	100	100	100	110	101
$\|101\rangle$	101	001	101	100	101	111	101
$\|110\rangle$	111	010	100	110	110	110	111
$\|111\rangle$	110	011	101	110	111	111	111

Fig. 10 Truth table for 2−CN gate impacted by measurement faults. The column denoted *input* shows the input combinations possible on the amplitude plane. Columns denoted *a–f* show the circuit's response given the presence of faults from Fig. 9a–f

Definition 8.1 Measurement fault model: A working measurement gate is replaced with a faulty measurement gate that returns only a *logic-zero* or a *logic-one*. (This is similar to the stuck-at fault model except here it's the measurement gate that is stuck, instead of a internal wire.)

Quantum Fault Model 7 (Measurement Fault Model) *Each qubit must be measured in both* logic-zero *and* logic-one *states.*

9 Conclusion

In this work we have considered the adaptation of know classical methods to test quantum circuits. The first step in this program is to develop a set of realistic quantum fault models. The fault models we have presented enable circuit testing at the logical, as oposed to currently practiced approach of testing quantum circuits at the

input	a	b	c	d	e	f
$\|000\rangle$	0	0	0	1	1	1
$\|001\rangle$	0	0	1	1	1	0
$\|010\rangle$	0	1	0	1	0	1
$\|011\rangle$	0	1	1	1	0	0
$\|100\rangle$	1	0	0	0	1	1
$\|101\rangle$	1	0	1	0	1	0
$\|110\rangle$	1	1	0	0	0	1
$\|111\rangle$	1	1	1	0	0	0

Fig. 11 Fault table for 2−CN gate derived from Fig. 9. Each binary entry in the fault table corresponds to a single test (*row*) and a single fault (*column*). Tests are labeled $|000\rangle$ to $|111\rangle$ and faults are labeled *a–f*. A value of *1* in the table corresponds to a given test (*row*) detecting (*covering*) a given fault (*column*)

device level. Finding additional fault models, that are physically inspired and not dominated by the those introduced here, is an open problem. In the Appendix we have included an example test set for a specfic circuit using the fault models presented in this work.

Acknowledgments The Quantum Circuit diagrams were drawn in LaTeX using Q-circuit [16]. The simulation tool QuIDDPro [55] was used during this study. We would like to thank G.F. Viamontes, D. Maslov, J.A. Jones and P.J. Love.

Appendix A: The Partial Trace

In this Appendix we review the partial trace [41]. Consider Hilbert space A of system $A \otimes B$. We will trace over system A, leaving system B in a mixed state. We have, $tr_A(|a_1\rangle \langle a_2| \otimes |b_1\rangle \langle b_2|)$. Now consider $|e_i\rangle$ as an orthonormal basis for system A, we may write the partial trace as, $\sum_i \langle e_i| a_1\rangle \langle a_2| \otimes |b_1\rangle \langle b_2| e_i\rangle$. After we recall the general fact about tensor products, $|a\rangle \langle b| \otimes |c\rangle \langle d| = |a\rangle |c\rangle \langle b| \langle d|$, it is easy to see a well known equation for the trace of a component part of a composite system, $\sum_i \langle e_i| a_1\rangle \langle a_2| e_i\rangle \otimes |b_1\rangle \langle b_2| = tr(|a_1\rangle \langle a_2|) |b_1\rangle \langle b_2|$.

Appendix B: Current Methods Used to Test Quantum Circuits

For the sake of completeness, in this Appendix we review the main approach currently used to test quantum circuits. By providing references and an introduction to current testing methods, this Appendix is designed to aid readers from other backgrounds who are working on the quantum test problem.

In the mid to late 90's experimentalists developed a method of black box characterization known as quantum process tomography [12]. A quantum process is described as a map between input and output quantum states, e.g. $\rho_{\text{out}} = \mathcal{E}(\rho_{\text{in}}) = \sum_j E_j \rho_{in} E_j^\dagger$, where the map $\mathcal{E}$ is a *quantum operation*[9] and the operators E_j are called operation elements.[10] Process tomography is a procedure used to reconstruct the behavior of a quantum network by performing state tomography on a set of initial states ρ_i that form an operator basis for the system in question [11].[11] The input states and measurement projectors in process tomography each form a basis for the set of $n-$qubit density matrices requiring $d^2 = 2^{2n}$ elements in each set [41], where d is the dimension of the Hilbert space. For a two-qubit gate $d^2 = 16$, resulting in 256 different settings of input states and measurement projectors. One of many possible input combinations (adapted from the optics experiment in [44]) forming an operator basis needed to characterize the space of two-qubit circuits is the following:[12]

$$\{|00\rangle, |01\rangle, |10\rangle, |11\rangle, |0+\rangle, |0y_-\rangle, |1y_-\rangle, |1+\rangle, |++\rangle, |y_+y_-\rangle, |y_+ +\rangle, |+y_+\rangle, |+1\rangle, |y_+1\rangle, |+0\rangle, |y_+0\rangle\}. \quad (6)$$

Of course there exist many possible choices for such a basis. In general however, for a system of n qubits the computational basis states $|0\rangle, ..., \left|2^{n-1}\right\rangle$ and superpositions $(|q\rangle \pm |r\rangle)/\sqrt{2}$ are prepared, where $q \neq r$ [40].

Given many copies of an experimental sample, state tomography is a procedure allowing one to reconstruct an arbitrary quantum state to a given accuracy. It requires a set of simple measurement operators that are products of Pauli matrices. The method relies on creating a set of orthogonal measurements and using the Hilbert-Schmidt inner product [41] to expand the state of ρ based on the average outcome of each measurement. A single qubit may be reconstructed as the following density matrix:

$$\rho = \frac{tr(\rho)\sigma_i + tr(\sigma_x\rho)\sigma_x + tr(\sigma_y\rho)\sigma_y + tr(\sigma_z\rho)\sigma_z}{2}. \quad (7)$$

[9] In this work we only consider the case where $\sum_j E_j E_j^\dagger = I$.

[10] A review of the properties of operation elements is given in Ch. 3 of the 1998 PhD Thesis by Nielsen [39].

[11] A purely mathematical discussion of process tomography is presented, all measurements are treated as yielding exact probabilities and all sources of error in those measurements are ignored. For experimental background see for example [44] and [21, 36]. Chapter 8 in Ref. [41] also has an introduction to both State and Process Tomography.

[12] Using the notation that: $(|y_+\rangle = |0\rangle + i|1\rangle$ and $|y_-\rangle = |0\rangle - i|1\rangle)$. The measurement projectors corresponding to this set of initial states adapted from the optics experiment given in [44] are: $\langle 00|, \langle 10|, \langle +1|, \langle y_-0|, \langle y_-1|, \langle 11|, \langle 01|, \langle 0-|, \langle 0y_-|, \langle y_-y_-|, \langle y_--|, \langle +-|, \langle +y_+|, \langle 1-|, \langle 1y_-|$ and $\langle +0|$.

Expressions like $tr(\sigma_x \rho)$ in Eq. 7 refer to an average measurement outcome where σ_x is an observable. A similar expansion to that of Eq. 7 applies to n–qubit systems. For example, reconstruction of any two-qubit operator requires a total of $2^{2n} = 16$ measurement observables:

$$\begin{aligned}\{&\sigma_i \otimes \sigma_i, \sigma_i \otimes \sigma_x, \sigma_i \otimes \sigma_y, \sigma_i \otimes \sigma_z, \sigma_x \otimes \sigma_i, \sigma_x \otimes \sigma_x,\\ &\sigma_x \otimes \sigma_y, \sigma_x \otimes \sigma_z, \sigma_y \otimes \sigma_i, \sigma_y \otimes \sigma_x, \sigma_y \otimes \sigma_y,\\ &\sigma_y \otimes \sigma_z, \sigma_z \otimes \sigma_i, \sigma_z \otimes \sigma_x, \sigma_z \otimes \sigma_y, \sigma_z \otimes \sigma_z\}. \end{aligned} \tag{8}$$

A difficulty associated with quantum process tomography is that in experimental practice, the observables are not easily realized. A system with d dimensions requires $16^d - 4^d$ independent parameters to uniquely describe the process [11], where $d = 2^n$. The useful method of quantum process tomography was developed out of a need for black box characterization (for that purpose its use appears unavoidable). However, process tomography works independently of the set of gates realized in the network and their possible faults and when used as a method to test quantum switching networks, it has a classical counterpart known as *brute-force* or complete *functional-testing*.

Distance measures between quantum states are now reviewed. First we recall the well known Fidelity measure between quantum states.

Definition B.1 The *Fidelity* between density matrices ρ and σ is defined as:

$$F(\rho, \sigma) \equiv tr\left(\sqrt{\sqrt{\rho}\sigma\sqrt{\rho}}\right)^2 \tag{9}$$

When $\rho = |\psi\rangle\langle\psi|$ is a pure state the fidelity has an easy interpretation as the overlap between ρ and σ, reducing to:

$$F(\psi, \sigma) = \langle\psi|\sigma|\psi\rangle.$$

Furthermore, the Fidelity evaluates to zero when two pure states being compared are orthogonal, it evaluates to one when two states being compared are identical, and is not a metric.[13] For a discussion regarding an operational interpretation of the Fidelity for a mixed state see [15].

A second common distance measure is the Trace Distance between quantum states.

Definition B.2 The *Trace Distance* between density matrices ρ and σ is defined as:

$$D(\rho, \sigma) \equiv \frac{1}{2} tr|\rho - \sigma| \tag{10}$$

where $|Z| = \sqrt{Z^\dagger Z}$. Since $0 \leq D \leq 1$ the trace distance is a genuine metric on quantum states [17, 41] and thus has the following three properties: (i) $D(\rho, \sigma) \geq 0$ with $D(\rho, \sigma) = 0$ *iff* $\sigma = \rho$, (ii) Symmetry: $D(\rho, \sigma) = D(\sigma, \rho)$, and (iii) the Triangle Inequality: $D(\mathcal{E}(\rho), \mathcal{G}(\rho)) \leq D(\mathcal{E}(\rho), \mathcal{F}(\rho)) + D(\mathcal{F}(\rho), \mathcal{G}(\rho))$. The Trace Distance represents the statistical distribution between quantum states with respect to measurement. The Trace Distance has the property of *contractivity*, $D(\mathcal{E}(\rho), \mathcal{E}(\sigma)) \leq D(\rho, \sigma)$ whenever $\mathcal{E}$ is a trace-preserving quantum operation. This just means that acting on arbitrary quantum states ρ and σ both with operation $\mathcal{E}$ will never increase how well one can distinguish these states with respect to measurements [17, 41].

The Trace Distance and Fidelity are complementary measures and should be considered equally important

[13] Two common ways of turning the Fidelity into a metric are the *Bures metric*, $B(\rho, \sigma) \equiv \sqrt{2 - 2\sqrt{F(\rho, \sigma)}}$ and the *angle*, $A(\rho, \sigma) \equiv \arccos\left(\sqrt{F(\rho, \sigma)}\right)$, a very comprehensive discussion of these details can be found elsewhere, e.g. [17].

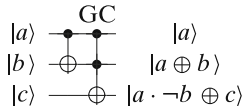

Fig. 12 Test example: gold circuit, or the ideal circuit that implements the specific functions on the output bits, as illustrated

abc	GC	f_1	f_2	f_3	f_4	f_5	f_6	f_7
000	000	010	000	000	000	000	000	000
001	001	011	001	001	001	001	001	001
010	010	000	011	010	010	010	010	010
011	011	001	010	011	011	011	011	011
100	111	111	111	101	100	111	110	110
101	110	110	110	100	101	110	111	111
110	100	100	100	111	100	111	100	101
111	101	101	101	110	101	110	100	101

Fig. 13 Truth table for the correct circuit (column GC see Fig. 12) to be compared with the circuit perturbed with the faults f_1 through f_7 (see Fig. 14)

when comparing two quantum states [17]. Distance measures may also be used to compare and contrast a real process $\mathcal{F}$ and an ideal process $\mathcal{E}$, such that $\Delta(\mathcal{F}, \mathcal{E})$ defines an error metric on a quantum process [17].

Definition B.3 The *S-Fidelity* between real quantum process $\mathcal{F}$ and ideal quantum process $\mathcal{E}$ is defined as:

$$\Delta^{F}_{\min}(\mathcal{F}, \mathcal{E}) \equiv \min_{|\psi\rangle} \Delta(\mathcal{F}(\psi), \mathcal{E}(\psi)) \tag{11}$$

where the minimum is over all possible pure state inputs and Δ is a Fidelity measure on quantum states.

Definition B.4 The *S-Distance* between real quantum process $\mathcal{F}$ and ideal quantum process $\mathcal{E}$ is defined as:

$$\Delta^{D}_{\max}(\mathcal{F}, \mathcal{E}) \equiv \max_{|\psi\rangle} \Delta(\mathcal{F}(\psi), \mathcal{E}(\psi)) \tag{12}$$

where the maximum is over all possible pure state inputs and Δ is a Distance metric on quantum states.

Instead of considering all pure states, it is helpful to restrict our thinking to a set of inputs needed to form a complete operator basis for the system in question. In this case, experimentally determining the S-Distance/S-Fidelity amounts to performing state tomography on this complete operator basis input set while keeping track of the worst Trace Distance (Eq. 10)/Fidelity (Eq. 9) between the reconstructed state and that of the ideal. [17] stated that, *...the S-Distance and S-Fidelity are the two best error measures, and should be used as the basis for comparison of real quantum information processing experiments to the theoretical ideal.*

Appendix C: Testing Example

In this section we will consider testing the correct circuit presented in Fig. 12. Figure 14 diagrammatically illustrates the quantum circuit perturbed by fault models we have considered and introduced thought this work. Readers can consult the table in Fig. 13 to consider a test set that will determine if fault models considered in this work are present in the circuit under test (Fig. 14).

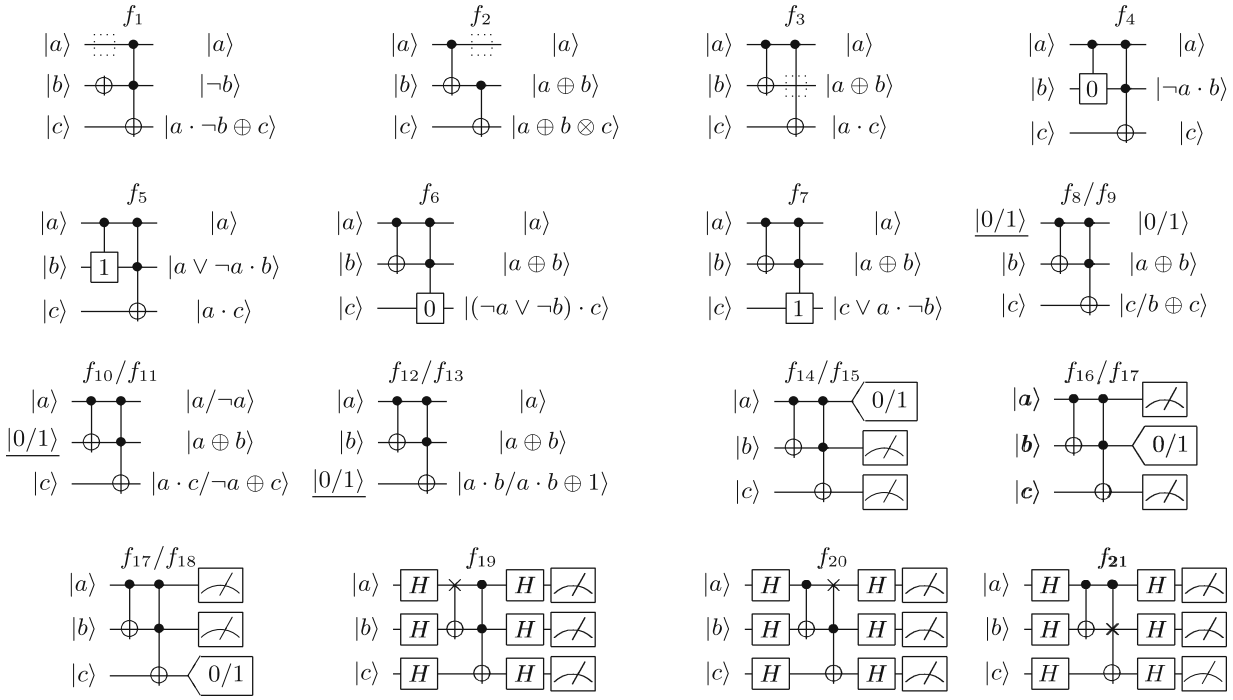

Fig. 14 Faults f_1, f_2 and f_3 illustrate missing control faults. Forced gate faults are depicted in f_4–f_7. Stuck input faults are illustrated in f_8–f_{13} and struck measurement faults are in f_{14}–f_{18}. Phase faults are illustrated in f_{19}–f_{21}. See Fig. 12 for the functional circuit and Fig. 13 for the truth table for the faults f_1–f_7

References

1. Aharonov D, Ben-Or M (1998) Fault-tolerant quantum computation with constant error rate. In: Proc 29th ann ACM symp on theory of computing, New York, p 176. quant-ph/9611025; quant-ph/9906129
2. Allen JS, Biamonte JD, Perkowski MA (2005) ATPG for reversible circuits using technology-related fault models. In: Proc 7th international symposium on representations and methodology of future computing technologies, RM2005, Tokyo, Japan, 5–6 September 2005, 8 pp
3. Amin MHS, Grajcar M, II'ichev' E, Maassen van den Bringk AM, Rose G, Smirnov AY, Zagoskin AM (2004) Superconducting quantum storage and processing. In: IEEE interational solid-state circuits conference, ISSCC, Session 16, 10 pp
4. Anwar MS, Bazina D, Carteret H, Duckett SB, Halstead TK, Jones JA, Kozak CM, Taylor RJK (2004) Preparing high purity initial states for nuclear magnetic resonance quantum computing. Phys Rev Lett 93:040501. quant-ph/0312014, 3 pp
5. Barenco A, Bennett CH, Cleve R, DiVincenzo DP, Margolus N, Shor PW, Sleator T, Smolin J, Weinfurter H (1995) Elementary gates of quantum computation. Phys Rev A 52(5):3457–3467. quant-ph/9503016, 31 pp
6. Barenco A, Brun TA, Schack R, Spiller TP (1998) Effects of noise on quantum error correction algorithms. Mod Phys Lett A 13:2503–2512. quant-ph/9612047
7. Bettelli S (2004) Quantitative model for the effective decoherence of a quantum computer with imperfect unitary operations. Phys Rev A 69:042310. quant-ph/0310152, 14 pp
8. Biamonte JD, Perkowski MA (2004) Testing a quantum computer. In: Proceedings of KIAS-KAIST 5th workshop on quantum information science, Seoul Korea, 29–31 August 2004, p 16
9. Bowdrey MD, Jones JA (2001) A simple and convenient measure of NMR rotor fidelity. JAJ-QP-01-01. quant-ph/0103060
10. Childs AM, Preskill J, Renes J (2000) Quantum information and precision measurement. J Mod Opt 47:155–176. quant-ph/9904021
11. Childs AM, Chuang IL, Leung DW (2001) Realization of quantum process tomography in NMR. Phys Rev A 64:012314. quant-ph/0012032, 8 pp
12. Chuang IL, Nielsen MA (1997) Prescrition for experimental determination of the dynamics of a quantum black box. J Mod Opt 44:2455. quant-ph/9610001, 6 pp
13. Cummins HK, Jones JA (2000) Use of composite rotations to correct systematic errors in NMR quantum computation. New J Phys 2:6.1–6.12. quant-ph/9911072, 11 pp
14. Cummins HK, Llewellyn G, Jones JA (2003) Tackling systematic errors in quantum logic gates with composite rotation. Phys Rev A 67:042308. quant-ph/0208092, 7 pp
15. Dodd JL, Nielsen MA (2002) A simple operational interpretation of the fidelity. Phys Rev A 66:044301. quant-ph/0111053, 1 p
16. Eastin B, Flammia ST (2004) Q-circuit tutorial. Free online, quant-ph/0406003, 7 pp
17. Gilchrist A, Langford NK, Nielsen MA (2005) Distance measures to compare real and ideal quantum processes. Phys Rev A 71:062310. quant-ph/0408063, 14 pp
18. Grover LK (2005) A different kind of quantum search. quant-ph/0503205, 13 pp
19. Hayes JP, Polian I, Becker B (2004) Testing for missing-gate faults in reversible circuits. In: Proc Asian test symposium, Taiwan, pp 100–105
20. Howard P (2004) Nuclear magnetic resonance quantum computation. In: Esteve D, Raimond J-M, Dalibard J (eds) Quantum entanglement and information processing. Elsevier. http://nmr.physics.ox.ac.uk
21. James DFV, Kwiat PG, Munro WJ, White AG (2001) On the measurement of qubits. Phys Rev A 64:052312. quant-ph/0103121, 21 pp
22. Jones JA (2001) NMR quantum computing. In: Quantum computation and quantum information theory. World Scientific, Singapore. http://nmr.physics.ox.ac.uk
23. Jones JA, Knill E (1999) Efficient refocussing of one spin and two spin interactions for NMR quantum computation. J Magn Reson 141:322–325. quant-ph/9905008
24. Jones JA, Mosca M (1998) Implementation of a quantum algorithm to solve Deutsch's problem on a nuclear magnetic resonance quantum computer. J Chem Phys 109:1648–1653. quant-ph/9801027
25. Jones J, Mosca M (1999) Approximate quantum counting on an NMR ensemble quantum computer. Phys Rev Lett 83:1050. quant-ph/9808056, 4 pp
26. Jones JA, Hansen RH, Mosca M (1998) Quantum logic gates and nuclear magnetic resonance pulse sequences. J Magn Reson 135:353–360. quant-ph/9805070
27. Jones J, Mosca M, Hansen R (1998) Implementation of a quantum search algorithm on a nuclear magnetic resonance quantum computer. Nature 393:344–346. quant-ph/9805069
28. Kak S (1999) The initialization problem in quantum computing. Found Phys 29:267–279. quant-ph/9805002
29. Kalay U, Perkowski MA, Hall DV (2000) A minimal universal test set for self-test of EXOR-sum-of-product circuits. IEEE Trans Comput 49(3):267–276
30. Kautz W (1961) Automatic fault detection in combinatoinal switching networks. In: Proc AIEE 2nd switching circuit theory and logical design symp, pp 195–214
31. Kautz WH (1971) Testing faults in combinational cellular logic arrays. In: Proceedings of 8th annu symp switching and automata theory, pp 161–174
32. Kim K, Song M, Lee S, Lee J-S (2005) Quantum process tomography with arbitary number of ancillary qubits in nuclear magnetic resonance. J Korean Phys Soc 47:736–739
33. Knill E, Laflamme R, Zurek WH (1997) Resilient quantum computation: error models and thresholds. In: Proc mathematical, physical engineering sciences, vol 454, pp 365–384. quant-ph/9702058
34. Knill E, Laflamme R, Ashikhmin A, Barnum H, Viola L, Zurek WH (2002) Introduction to quantum error correction. LA Science 27:188–225. quant-ph/0207170, 22 pp
35. Lee S, Lee JS, Kim T, Biamonte JD, Perkowski MA (2005) The cost of quantum gate primitives. J Mult-Valued Log Soft Comput
36. Leung DW (2000) Towards robust quantum computation. PhD Dissertation, Stanford University, July 2000. cs/0012017, 243 pp
37. Maslov D, Young C, Miller DM, Dueck GW (2005) Quantum circuit simplification using templates. In: Proc DATE conference, Munich, Germany, pp 1208–1213
38. McCluskey EJ, Tseng CW (2000) Stuck-fault tests vs actual defects. In: Proc 2000 int test conf, Atlantic City, pp 336–343
39. Nielsen MA (1998) Quantum information theory. PhD thesis, University of New Mexico, Report UNM-98-08. quant-ph/0011036, 259 pp

40. Nielsen MA (2002) A simple formula for the average gate fidelity of a quantum dynamical operation. Phys Lett A 303(4):249–252. quant-ph/0205035
41. Nielsen MA, Chuang IL (2000) Quantum computation and quantum information. Cambridge University Press
42. Obenland KM, Despain AM (1996) Impact of errors on a quantum computer architecture. Technical report, Information Sciences Institute, University of Southern California, 1 October 1996. http://www.isi.edu/
43. O'Brien JL, Pryde GJ, White AG, Ralph TC, Branning D (2003) Demonstration of an all-optical quantum controlled-NOT gate. Nature 426:264. quant-ph/0403062, 5 pp
44. O'Brien JL, Pryde GJ, Gilchrist A, James DFV, Langford NK, Ralph TC, White AG (2004) Quantum process tomography of a controlled-NOT gate. Phys Rev Lett 93:080502. quant-ph/0402166, 4 pp
45. Oskin M (2004) Quantum computing lecture notes. Class notes, University of Washington. cs.washington.edu
46. Patel KN, Hayes JP, Markov IL (2004) Fault testing for reversible circuits. IEEE Trans CAD 23(8):1220–1230. quant-ph/0404003
47. Perkowski MA et al (2005) Test generation and fault localization for quantum circuits. In: Proc 35th ISMVL, pp 62–68. doi:10.1109/ISMVL.2005.46
48. Reichardt BW, Grover LK (2005) Quantum error correction of systematic errors using a quantum search framework. Available online at quant-ph/0506242, 6 pp
49. Shenvi N, Brown KR, Whaley KB (2003). Effects of random noisy oracle on search algorithm complexity. Phys Rev A 68:052313 quant-ph/0304138, 11 pp
50. Shor PW (1996) Fault-tolerant quantum computation. In: 37th symposium on foundations of computing, vol 37. IEEE Computer Society Press, pp 56–65. quant-ph/9605011
51. Shukla SK, Kam R, Goldstein SC, Brewer F, Banejee K, Basu S (2003) Nano, quantum, and molecular computing: are we ready for the validation and test challenges? In: IEEE pannel disscussion, 0-7803-8236-6, pp 3–7. http://www.ece.ucsb.edu/
52. Steane AM, Lucas DM (2000) Quantum computing with trapped ions, atoms and light. Fortschr Phys (special issue). quant-ph/0004053, 17 pp
53. Steffen M, Vandersypen LMK, Chuang IL (2001) Toward quantum computation: a five-qubit quantum processor. IEEE MICRO 21(2):24–34. doi:10.1109/40.918000
54. Vandersypen LMK, Yannoni CS, Chuang IL (2002) Liquid state NMR quantum computing. In: Encyclopedia of nuclear magnetic resonance, vol 9. Advances in NMR, pp 687–697. http://qt.tn.tudelft.nl
55. Viamontes GF, Markov IL, Hayes JP (2005) Graph-based simulation of quantum computation in the density matrix representation. Quantum Information and Computation 5(2):113–130
56. White AG, Gilchrist A, Pryde GJ, O'Brien JL, Bremner MJ, Langford NK (2003) Measuring controlled-NOT and two-qubit gate operation. quant-ph/0308115, 10 pp
57. Williams CP, Clearwater SH (1998) Explorations in quantum computing. Springer
58. Xiao L, Jones JA (2005) Error tolerance in an NMR implementation of Grover's fixed-point quantum search algorithm. Phys Rev A 72:032326. doi:10.1103/PhysRevA.72.032326
59. Zurek WH (1984) Reversibility and stability of information processing systems. Phys Rev Lett 53:391–394. doi:10.1103/PhysRevLett.53.391

Jacob D. Biamonte is a Research Fellow at the University of Oxford and a Lecturer in Physics at St. Peter's College.

Jeff S. Allen currently works in industry and was a graduate student at Portland State University when completing this work.

Marek A. Perkowski is Professor of Electrical Engineering at Portland Sate University.